

Electron Cooling Friction Force—Comparison of Different Approaches

I. N. Meshkov^{1,2,1)}

¹ Joint Institute for Nuclear Research, Dubna, Russia,

² Saint-Petersburg University, Saint-Petersburg, Russia.

Abstract: The theory of the electron cooling method has been under development since the first proposal of the method by G. I. Budker in 1996. A brief description of the development of the electron cooling method and its theory is given in this work. The main attention is paid to a new approach to the rigorous solution of the electron–ion interaction in binary collisions. The derived formulas for the cooling friction force are compared with the well-known empirical formula developed by V. Parkhomchuk at the end of the 1970s. The main problems of further development and application of the electron cooling theory are briefly considered in the conclusion.

Key words: electron, ion, collisions, Coulomb logarithm, friction force

PACS: 29.20.-c, 29.20.Dh, 29.27.-a

Foreword: Half a Century of the Electron Cooling Method

Fifty years ago G. Budker formulated the principle of the electron cooling method at The Symposium at Saclay (France) and later published it in the *Atomic Energy* journal [1]. Budker’s proposal was based on the model of the electron-proton Maxwellian plasma, and it was actually a “trigger” for many years’ “race” of the electron cooling method development. In 1968 the first prototype of the electron cooler was commissioned [2], and in 1970 the first electron cooler started up [3], which was soon used in the first experiments on electron cooling of protons at the NAP-M storage ring [4]. Since the first successful experiment and until now *21 electron coolers* have been constructed. Some of them are put out of operation, and some are under design and/or construction.

Introduction: status of the electron cooling theory

Budker’s proposal was based on the model of the electron-proton Maxwellian plasma. First doubts appeared as a result of the experimental discovery of the so-called “fast electron cooling”, when the cooling time measured experimentally was found to be much shorter than predicted by the theory: about 20 ms instead of 1 s [5]. This result was soon explained by the effects of the so-called “flattened distribution” of cooling electrons (see, for instance, Ref. 6) and “magnetization” of electrons in the electron beam travelling in a longitudinal magnetic field [7]. Correspondingly, the theory of the

electron cooling method was significantly developed from Budker’s plasma model to the model of the magnetized electron beam with a flattened Maxwellian distribution of electrons over velocities [8]. Simultaneously, a phenomenological formula—so called *Parkhomchuk formula* [6, 9]—for the electron cooling friction force was developed on the basis of the analysis of the experimental results obtained at NAP-M. The formula was tested in several experiments at different storage rings [10], compared with the results of the numerical experiments [11], and confirmed by all of them. It appeared to be more convenient than the formulas derived theoretically (see Ref. 8). Its only disadvantage is absence of a theoretical basis, although

1) Email: meshkov@jinr.ru

some qualitative considerations and argumentations were presented [6, 9].

Concerning the efforts of the theoretical approach to the derivation of the cooling friction force formula, one should mention some confusion with the formulas from Ref. 7 that have been found recently [12]. The corrected formulae have the following form:

$$\vec{F}_\perp = -\frac{Q}{2} \cdot \frac{(V_\perp^2 - 2V_\parallel^2)L^A + 6V_\parallel^2}{V^2} \cdot \frac{\vec{V}_\perp}{V^3},$$

$$\vec{F}_\parallel = -\frac{Q}{2} \left(3L^A \frac{V_\perp^2}{V^2} + 2 \frac{V_\parallel^2 - 2V_\perp^2}{V^2} \right) \cdot \frac{\vec{V}_\parallel}{V^3}.$$

In Ref. 7 the term $6V_\parallel^2$ in formula (13) for F_\perp and the term $V_\parallel^2 - 2V_\perp^2/V^2$ in formula (14) for F_\parallel are missing. Unfortunately, these formulas were quoted in many articles (including Refs 6, 8, 9). Such an unpleasant, to some extent, fact makes it only more urgent to develop the electron cooling theory.

In this paper we make an attempt to give a theoretical formulation of the electron cooling friction force based on a rigorous consideration of *binary electron-ion collisions*. We analyze an idealized (“simplified”) case of an electron cooler with an absolutely homogeneous magnetic field in the cooling section with the power supply devoid of any voltage/current fluctuations and electron gun aberrations. We do not consider diffusion processes in the ion beam (ion diffusion on cooling electrons, intrabeam scattering in the ion beam, ion scattering on residual gas atoms, etc.) and restrict ourselves to the description of the cooling friction force as a function of the ion and electron velocities.

1 Cooling friction force in Rutherford scattering

The simplest case where the electron cooling friction force appears is a collision of free electrons and ions. Such collisions lead to momentum transfer from one particle to another. In the ion reference system the process looks like an electron wind that blows on the ion and pushes it in the direction opposite to the instant velocity of the ion.

To calculate the cooling (“friction”) force, we begin with consideration of free electron-ion collisions. It is a

particular case of the classical *two-body problem*, when the particles (“bodies”) interact via the central Coulomb force. This interaction is described in the centre-of-mass system of two colliding particles by the equation (see details in the Annex I)

$$\mu \ddot{\vec{r}} = -\frac{Ze^2}{r^3} \cdot \vec{r}, \quad \mu = \left(\frac{1}{m} + \frac{1}{M} \right)^{-1}, \quad (1.1)$$

where μ is the so-called “reduced mass”, e and Ze are the electric charges of the electron and the ion, m and M are their masses, \vec{r} is the radius-vector between the colliding ion and electron (Fig. 1). The relative velocity of the electron and the ion is

$$\dot{\vec{r}} = \vec{V} - \vec{v} \equiv \vec{U}(t), \quad (1.2)$$

where \vec{V} and \vec{v} are the ion and electron velocities in the reference frame moving with the average velocity of the ions to be cooled and the cooling electrons—the *particle reference frame* (PRF). Therefore, we can consider the case of nonrelativistic velocities \vec{V} and \vec{v} . In the PRF the average velocities of the ions and electrons are $\langle \vec{V} \rangle = \langle \vec{v} \rangle = 0$.

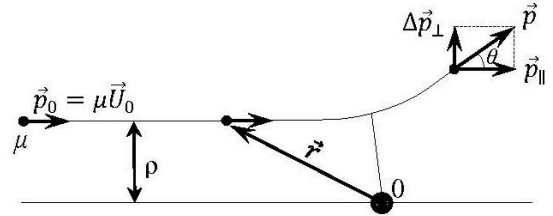


Fig. 1 Charged particle in a central Coulomb field; μ , \vec{p}_0 , \vec{p} are the mass and momentum of the μ -particle, \vec{r} is its radius-vector, ρ is the so-called impact parameter, θ is the scattering angle, and O is the field center.

Equation (1.1) can be integrated rigorously [13] that gives us the value of the scattering angle θ

$$\theta = 2 \arctan \frac{Ze^2}{\rho \mu U_0^2} \approx \frac{2Ze^2}{\rho \mu U_0^2} \quad \text{at } \theta \ll 1. \quad (1.3)$$

Here $\vec{U}_0 \equiv \vec{U}(0)$. The last expression for θ is written in the approximation of small-angle scattering that prevails in the electron cooling process. After averaging over many collisions at the given impact parameter ρ we obtain the momentum change of the μ -particle

$$\langle \Delta p_\parallel \rangle = p_0(1 - \cos \theta) \approx \frac{2Z^2 e^4}{\rho^2 \mu U_0^3}, \quad \langle \Delta p_\perp \rangle = 0. \quad (1.4)$$

The subscripts \parallel and \perp mark the momentum components parallel and perpendicular to the vector \vec{U}_0 . According to formula (I.8) in Annex I, it is equal to the momentum transfer from the colliding electron to the ion. Now, integrating over the electron velocity distribution and impact parameters ρ in the range $\rho_{min} \leq \rho \leq \rho_{max}$, one can write a formula for the cooling friction force for free binary collisions

$$\begin{aligned}\vec{F}_{free}(\vec{V}) &= -\langle \Delta \vec{p}_{\parallel} \rangle \cdot \frac{dN_{collision}}{dt} = \\ &= -n_e \int_{\vec{v}} \vec{U}_0(\vec{V}, \vec{v}) f(\vec{v}) d^3v \times \\ &\times 2\pi \int_{\rho_{min}}^{\rho_{max}} \rho \cdot d\rho \cdot \langle \Delta p_{\parallel} \rangle,\end{aligned}\quad (1.5)$$

The symbol $\int_{\vec{v}} d^3v$ denotes here and below a triple integral over the electron velocity \vec{v} ($d^3v = dv_x \cdot dv_y \cdot dv_z$), n_e is the electron density in the PRF, $f(\vec{v})$ is the electron velocity distribution there. Substitution of $\langle \Delta \vec{p}_{\parallel} \rangle$ (1.4) into (1.5) gives us

$$\vec{F}_{free} = -QL_{free} \int_{\vec{v}} \frac{\vec{V} - \vec{v}}{|\vec{V} - \vec{v}|^3} \cdot f(\vec{v}) d^3v, \quad (1.6)$$

$$Q = \frac{4\pi Z^2 e^4 n_e}{m} = 4\pi (Zr_e c)^2 n_e \cdot mc^2, \quad L_{free} = \ln \frac{\rho_{max}}{\rho_{min}}.$$

Here r_e is the classical electron radius, and we take into account the approximate value of the reduced mass

$$\mu \approx m \text{ at } m \ll M.$$

The dimension of the Q parameter is $[Q] = \text{eV} \cdot \text{cm} \cdot \text{s}^{-2}$. L_{free} is the so-called Coulomb logarithm at free collisions. The impact parameter ρ_{max} depends on several characteristics of the electron cooler. The first is the electron density in the cooling electron beam and the related effect of the well-known Debye screening [14]: the electric field of an ion inserted into an electron cloud vanishes with the distance from the ion as

$$\varphi(r) = \frac{eZ}{r} \cdot e^{-r/R_D}, \quad R_D = \sqrt{\frac{T_e}{4\pi n_e e^2}}.$$

The symbol R_D is the so-called “Debye radius”. In our case electrons move relative to the ion with velocity \vec{U} (1.2). Therefore, electrons have one strongly pronounced component of their temperature: $T_e = mU^2$ ($U \equiv |\vec{U}|$),

and the formula for R_D can be rewritten as

$$R_D = \frac{U}{\omega_e}, \quad \omega_e = \sqrt{\frac{4\pi n_e e^2}{m}}, \quad (1.7)$$

the so-called electron plasma frequency. In addition, the number of electrons has to be sufficiently large inside the sphere of the radius R_D , i.e., the *neutralization radius*

$$R_z = \left(\frac{3Z}{4n_e} \right)^{1/3} \quad (1.8)$$

has to be smaller than R_D . Thus,

$$\rho_{max}^{(1)} \leq R_{shield} \equiv \max(R_D, R_z). \quad (1.9)$$

The second effect is the relation between the collision duration and the time of electron travelling in the PRF through the cooling electron system

$$\tau_{collision} \sim \frac{\rho}{U} \leq \tau_{flight} = \frac{L_0}{\gamma \beta c}.$$

Here L_0 is the length of the cooling section, $\beta = V_0/c$, $\gamma = (1 - \beta^2)^{-1/2}$. This gives us

$$\rho_{max}^{(2)} \leq R_{flight} = \frac{L_0 U}{\gamma \beta c}. \quad (1.10)$$

The third effect is obvious: an impact parameter cannot exceed the transverse electron beam size a_e . Summing all three effects we obtain

$$\rho_{max} = \min\{R_{shield}, R_{flight}, a_e\}. \quad (1.11)$$

The parameter ρ_{min} can be estimated from the condition of the μ -particle scattering by the angle $\pi/2$

$$\rho_{min} = \frac{Ze^2}{mU^2}. \quad (1.12)$$

Formula (1.6) has the same structure as the formula for the Coulomb force acting on the electric charge $q = QL_{free}$ inside the system of the electric charges of the density $\rho(\vec{r}) = f(\vec{v})$; the position of the charge q is described by the radius vector $\vec{R} = \vec{V}$ and by the position of an element of the charge system—the radius vector $\vec{r} = \vec{v}$. Such a “Coulomb analogy” allows one to apply electrostatic field calculation methods to the calculation of the cooling friction force. For instance, an electron beam with a velocity distribution in the form of a disk of homogeneous density in the velocity space [8]

$$f_{flat}(\vec{v}) = \begin{cases} n_e, & -\Delta_{\parallel} \leq |v_{\parallel}| \leq \Delta_{\parallel}, \quad -\Delta_{\perp} \leq |v_{\perp}| \leq \Delta_{\perp}, \\ 0, & \Delta_{\parallel} < |v_{\parallel}|, \quad \Delta_{\perp} < |v_{\perp}|, \end{cases} \quad (1.13)$$

produces the cooling friction force that can be calculated by the “Gauss theorem” applied to the velocity space

$$F_{\perp} = -V_{\perp} Q L_{free} \begin{cases} U^{-3}, \\ \Delta_{\perp}^{-3}, \\ 0, \end{cases}$$

$$F_{\parallel} = -V_{\parallel} Q L_{free} \begin{cases} V^{-3}, & \Delta_{\perp} < U, \\ (|\vec{V}_{\parallel}| \cdot \Delta_{\perp}^2)^{-1}, & \Delta_{\parallel} < U < \Delta_{\perp}, \\ (\Delta_{\parallel} \Delta_{\perp}^2)^{-1}, & U < \Delta_{\parallel}. \end{cases} \quad (1.14)$$

In this case the subscripts “ \parallel ” and “ \perp ” indicate the directions along and across the velocity of the PRF.

However, the approximation of a “homogeneous disk” is very rough and gives only a qualitative description of the cooling friction force dependence on the ion velocity. A much more correct result corresponding to physical reality is obtained by using the function $f_{Maxw}(\vec{v})$ in the form of the *flattened Maxwellian distribution* in the PRF. For an axially symmetric electron beam it is [8]

$$f_{Maxw}(\vec{v}) d^3 \vec{v} = \left(\frac{m}{2\pi} \right)^{3/2} \frac{1}{T_{\perp} \sqrt{T_{\parallel}}} \times$$

$$\times \exp \left\{ - \left(\frac{mv_{\perp}^2}{2T_{\perp}} + \frac{mv_{\parallel}^2}{2T_{\parallel}} \right) \right\} \cdot 2\pi v_{\perp} \cdot dv_{\perp} \cdot dv_{\parallel}, \quad (1.15)$$

$$T_{\parallel} = \frac{T_{cathode}^2}{\beta^2 \gamma^2 m c^2} + e^2 n_e^{1/3},$$

$$T_{\perp} = T_{cathode} + T_{aberration}.$$

Here

$$T_{\perp} = m \langle v_{\perp}^2 \rangle \equiv m \Delta_{\perp}^2, \quad T_{\parallel} = m \langle v_{\parallel}^2 \rangle \equiv m \Delta_{\parallel}^2$$

are the temperatures corresponding to the transverse (v_{\perp}) and longitudinal (v_{\parallel}) components of the electron velocity relative to the electron beam axis in the PRF, $T_{cathode}$ is the temperature of the electron gun cathode, and $T_{aberration}$ is the contribution to the electron transverse temperature from the aberrations of the electron gun optics, perturbations of the magnetic field of the electron cooler, etc.

Analytic calculation of the cooling friction force by formula (1.6) for $f_{Maxw}(\vec{v})$ is a very hard task, if possible at all. Nevertheless, there is a “trick” that the author borrowed from the paper of Alexander Shemyakin [15], where he used the approach of Valery Lebedev (private communication, Fermilab), who adopted for the cooling process the simulation of the method developed by J. Bjorken and S. Mtingwa [16] for solving a very different problem.

The procedure is the following. First, we introduce the potential function for the cooling friction force (1.6):

$$\Phi(\vec{V}) = -Q L_{free} \int_{\vec{v}} \frac{f(\vec{v})}{|\vec{V} - \vec{v}|} \cdot d^3 \vec{v} \quad (1.16)$$

and consider a general case of the 3D electron distribution devoid of axial symmetry:

$$|\vec{V} - \vec{v}| = \sqrt{\sum_{\alpha=1}^3 (V_{\alpha} - v_{\alpha})^2}, \quad \alpha = x, y, s; \quad v_s \equiv v_{\parallel}. \quad (1.17)$$

Using the equality

$$\frac{1}{\sqrt{\sum_{\alpha=1}^3 (V_{\alpha} - v_{\alpha})^2}} = \frac{2}{\sqrt{\pi}} \int_0^{\infty} \exp\{-\xi^2 \sum_{\alpha=1}^3 (V_{\alpha} - v_{\alpha})^2\} \cdot d\xi, \quad (1.18)$$

we write formula (1.16) as follows:

$$\Phi(\vec{V}) = -\frac{Q L_{free}}{\sqrt{2\pi^2} \Delta_x \Delta_y \Delta_s} \int_0^{\infty} d\xi \int d^3 \vec{v} \times$$

$$\times \exp \left\{ -\sum_{\alpha=1}^3 \left[\xi^2 (V_{\alpha} - v_{\alpha})^2 + \frac{v_{\alpha}^2}{2\Delta_{\alpha}^2} \right] \right\}.$$

Transforming the terms in the square brackets to the square of the sum, we obtain the integrable expression and have

$$\Phi(\vec{V}) = -\frac{2Q L_{free}}{\sqrt{\pi}} \cdot \int_0^{\infty} \Pi_{\alpha=1}^3 \frac{1}{\sqrt{1+2\Delta_{\alpha}^2 \xi^2}} \cdot e^{\psi(\xi, \vec{V})} d\xi$$

$$\psi(\xi, \vec{V}) = \sum_{\beta=1}^3 \frac{\xi^2 v_{\beta}^2}{1+2\Delta_{\beta}^2 \xi^2}. \quad (1.19)$$

From the function $\Phi(\vec{V})$ we find the components of the cooling friction force

$$F_{\gamma}(\vec{V}) = -\frac{\partial \Phi(\vec{V})}{\partial V_{\gamma}} = \quad (1.20)$$

$$= -\frac{4Q L_{free}}{\sqrt{\pi}} \cdot V_{\gamma} \cdot \int_0^{\infty} \frac{\xi^2}{1+2\Delta_{\gamma}^2 \xi^2} \Pi_{\alpha=1}^3 \frac{1}{\sqrt{1+2\Delta_{\alpha}^2 \xi^2}} \cdot e^{\psi(\xi, \vec{V})} d\xi.$$

Thus, we have obtained the formula for the cooling

friction force that allows us to use a simple code for numerical simulations.

2 Electron cooling in magnetic field

2.1 Electron-ion collisions in magnetic field

We consider now a collision of an ion with an electron that travels along the magnetic field line and will deduce equations of motion of the cooling electron and the ion in the PRF (Fig. 2).

In electron coolers the magnetic field \vec{B} is relatively weak, i.e., the ion does not “feel” its influence

$$M\ddot{\vec{r}}_i = \frac{Ze^2}{r_{ie}^3} \cdot \vec{r}_{ie}, \quad (2.1)$$

but the electron is strongly influenced by both the magnetic field and the Coulomb field of the ion

$$m\ddot{\vec{r}}_e = -\frac{e}{c} [\dot{\vec{r}}_e, \vec{B}] - \frac{Ze^2}{r_{ie}^3} \cdot \vec{r}_{ie}. \quad (2.2)$$

The signs of the terms in equations (2.1) and (2.2) are chosen according to the signs of the electron and ion charges. The subscripts denote parameters related to the ion (“i”) or the electron (“e”). The radius vectors of both particles are defined in Fig. 2, \vec{v}_c is the velocity of the “Larmor circle” center directed along the magnetic field line. The vectors \vec{r}_i and \vec{r}_e are radius-vectors of the ion and the electron in the PRF, the symbols Ze and $-e$ indicate the ion and electron positions before collisions, 0 is the origin of the x , y , and s coordinates, the s axis is directed along the magnetic field \vec{B} , \vec{r}_c is the radius-vector of the center of the electron Larmor circle, \vec{r}_\perp is the radius-vector from the Larmor circle center to the electron, \vec{v}_c is the center velocity, \vec{r} is the vector from the ion to the circle center, the position of the x axis is chosen in the plane (\vec{v}_s, \vec{r}_i) , therefore the \vec{r} vector lies in the plane (x, s) ; the y axis is orthogonal to this plane; the dashed red arrow shows the initial direction of the ion velocity.

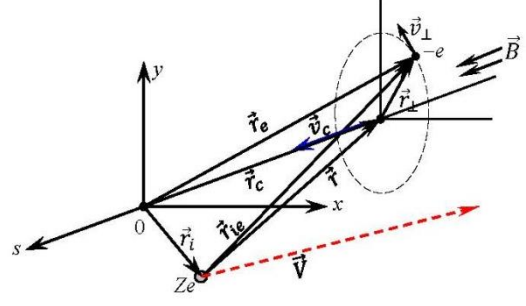


Fig. 2. The scheme of an ion collision with a magnetized electron (see explanation in the text).

Now we have to change again the definition of the longitudinal and transverse directions. The former is parallel to the magnetic field vector \vec{B} , and the latter is perpendicular to it.

From Fig. 2 we find

$$\vec{r}_{ie} = -\vec{r}_i + \vec{r}_e = \vec{r} + \vec{r}_\perp, \quad (2.3)$$

$$\vec{r}_e = \vec{r}_c + \vec{r}_\perp \quad (2.4)$$

$\vec{r}_\perp = \{x, y\}$, x , y , and s are the instant values of the electron coordinates. Introducing the electron Larmor rotation parameters

$$\rho_L = \frac{mv_{\perp}c}{eB}, \text{ electron Larmor radius,} \quad (2.5)$$

$$\omega_L = \frac{eB}{mc}, \text{ electron Larmor frequency,} \quad (2.6)$$

one can derive from (2.1)–(2.3) the following equation:

$$\ddot{\vec{r}}_{ie} = -\omega_L [\dot{\vec{r}}_e, \vec{e}_s] - \frac{Ze^2}{\mu r_{ie}^3} \cdot \vec{r}_{ie}. \quad (2.7)$$

Here \vec{e}_s is a unit vector directed along the magnetic field \vec{B} . Evidently,

$$[\dot{\vec{r}}_e, \vec{e}_s] = [\dot{\vec{r}}_\perp, \vec{e}_s] \equiv [\vec{v}_\perp, \vec{e}_s]. \quad (2.8)$$

Electron-ion collisions in a magnetic field can be analyzed using equation (2.7) with $\vec{r}_{ie} = \vec{r} + \vec{r}_\perp$ from (2.3) and equality (2.8). Then equation (2.7) falls into two ones:

$$\ddot{\vec{r}} = -\frac{1}{\mu} \cdot \frac{Ze^2}{r_{ie}^3} \vec{r}, \quad (2.9)$$

$$\ddot{\vec{r}}_\perp = -\omega_L [\dot{\vec{r}}_\perp, \vec{e}_s] - \frac{Ze^2}{\mu r_{ie}^3} \cdot \vec{r}_\perp. \quad (2.10)$$

The first peculiarity of collisions in a magnetic field is the existence of the range of free collisions at small impact

parameters. As follows from equation (2.7) or (2.10), the influence of the magnetic field on the electron motion vanishes if

$$\omega_L v_\perp \ll \frac{Ze^2}{\mu r_{ie}^3} \cdot \rho_L.$$

Here we used the identity $\dot{\vec{r}}_\perp = \vec{v}_\perp$; both vectors mean the transverse component of the electron velocity \vec{v} . This gives us the criterion (*the necessary condition*) for existence of free collisions:

$$\rho \sim r_{ie} \ll \left(\frac{Ze^2}{m\omega_L^2} \right)^{1/3} \equiv \rho_{crit}. \quad (2.11)$$

We illustrate this condition in Section 3.

Obviously, free collisions exist if $\rho_{crit} > \rho_{min}$. Together with formula (1.12) for ρ_{min} it gives us *the sufficient condition*:

$$U > U_{crit} = (Zr_e c^2 \omega_L)^{1/3}. \quad (2.12)$$

Note that condition (2.12) is always met in magnetic fields below several kG because the minimal value of U corresponds to $V = 0$, i.e., $U_{min} \sim v_\perp \sim \Delta_\perp$, and condition (2.12) can be written as

$$\frac{Zr_e c^2 \omega_L}{\Delta_\perp^3} < 1.$$

At $B = 1$ kG and $T_\perp = 0.1$ eV the left side of this inequality is of the order of $2 \cdot 10^{-3}$ Z.

We can conclude now that the free electron-ion collisions described in Section 1 exist in a magnetic field in the entire ion velocity range at low impact parameters $\rho < \rho_{crit}$. However, at higher impact parameters $\rho \geq \rho_{crit}$ the colliding electrons are “magnetized”.

On other hand, magnetized collisions disappear with decreasing magnetic field when ρ_{crit} approaches the ρ_{magn} value. The equality of these impact parameters gives us the criterion of the minimum magnetic field for magnetized collisions

$$B > B_{min} = \sqrt{\frac{Ze^2}{\rho_{magn}^3 r_e}}. \quad (2.13)$$

Displacement of a magnetized electron across the magnetic field is very small. It actually follows from equations (2.9) and (2.10) if we assume $r_{ie} = r \sim \rho$ and rewrite these equations as follows:

$$\ddot{\vec{r}} = -\frac{1}{\mu} \cdot \frac{Z^2}{r^3} \cdot \vec{r}, \quad (2.14)$$

$$\ddot{\vec{r}}_\perp = -\omega_L [\dot{\vec{r}}_\perp, \vec{e}_s] - \frac{Ze^2}{\mu \rho^3} \cdot \vec{r}_\perp. \quad (2.15)$$

For equation (2.15) the choice of r_{ie} equal to ρ is the upper limit. Equation (2.15) can be solved analytically (see details in Annex II). The electron trajectory (Fig. 3) found from (2.15) has a form of a spiral with the outer radial size (Annex II, formula (II.8))

$$r(t) = r_0 \sqrt{1 + \frac{4\omega_z^2}{\Omega^2} \cdot \sin^2 \frac{\Omega t}{2}},$$

$$\omega_z = \left(\frac{Ze^2}{m\rho^3} \right)^{1/2}, \quad \Omega = \sqrt{\omega_L^2 + 4\omega_z^2}. \quad (2.16)$$

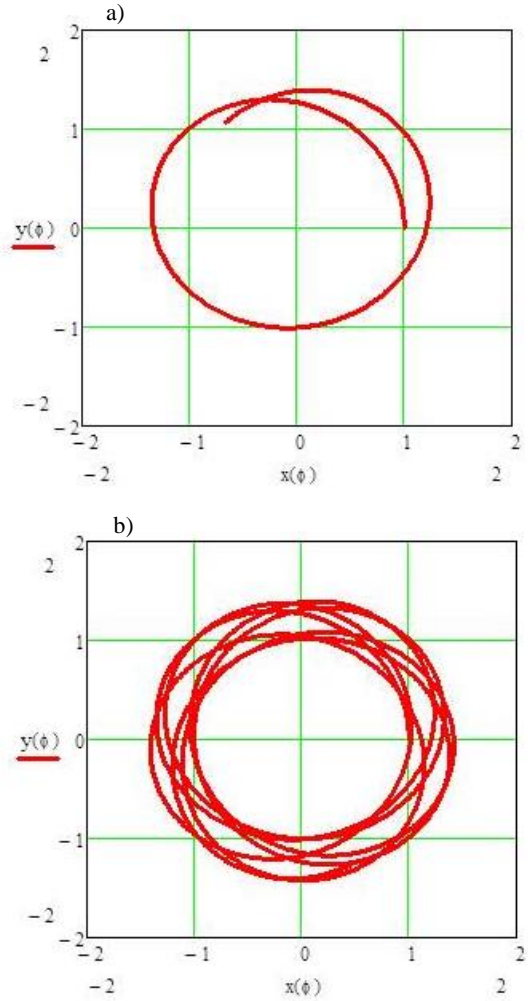


Fig. 3 The electron trajectory in the (x, y) plane, arbitrary units; n is the number of turns, $\phi = 2n\pi$: a) $n = 1$; b) $n = 5$, $x_0 = \rho_L = 1$, $y_0 = 0$, $v_x^0 = 0$, $v_y^0 = 1$, $\omega_z/\omega_L = -0.366$, $\omega_L/\Omega = 0.577$ (arbitrary units). The frequencies ω_\pm , ω_L and Ω (see Annex II) are calculated at $B = 1.0$ kG.

It means that when an electron and an ion collide at impact

parameters $\rho > \rho_{crit}$, the character of their interaction changes drastically: the electron is “bound” to the magnetic field line and travels along this line. The center of the electron Larmor circle does not displace across the field B line, but the electron transverse velocity oscillates in time (formula (II.12)), and its time-averaged value differs from the initial value v_{\perp}^0 by the factor

$$\Delta v_{\perp} = \sqrt{v_{\perp}^2} - v_{\perp}^0 = \left(\sqrt{1 + \frac{2\omega_z^4}{\omega_L^2(\omega_L^2 + 4\omega_z^2)}} - 1 \right) \cdot v_{\perp}^0. \quad (2.17)$$

This change in the electron transverse velocity in a collision gives us an estimate of the momentum transfer. However, due to the electron Larmor rotation, the electron and the ion come near each other N_{ρ} times during the collision time ρ/U_{magn}

$$N_{\rho} = \begin{cases} N_{turn} = \frac{\rho}{U_{magn}} \cdot \frac{\omega_L}{2\pi}, & \text{if } N_{turn} > 1, \\ 1 & \text{if } N_{turn} \leq 1. \end{cases} \quad (2.18)$$

Therefore, momentum transfer (2.19) is N_{ρ} times larger than that in a single collision:

$$(\Delta p_{\mu})_{\perp} = N_{\rho} \cdot \mu \Delta v_{\perp}. \quad (2.19)$$

We give numerical estimates of N_{ρ} in Section 3, Fig. 5. Using expressions for ω_z (II.2 in Annex II) and ρ_{crit} (2.12), we can write Δv_{\perp} in the following form:

$$N_{\rho} \cdot \Delta v_{\perp} = \delta_{\perp} v_{\perp}^0, \quad (2.20)$$

$$\delta_{\perp} = \frac{\omega_L \rho_{crit}}{2\pi U_{magn}} \cdot \left(\sqrt{1 + \frac{2}{\zeta^3(\zeta^3 + 4)}} - 1 \right), \quad \zeta = \frac{\rho}{\rho_{crit}}.$$

This result is used below (formulas (2.21), (2.24), (2.25)).

2.2 Friction force at magnetized collisions

Equation (2.14) has the form of the classical equation of the two-body problem (Annex I). Therefore, repeating the procedure described in Section 1, we arrive at a formula similar to (1.6), where relative electron-ion velocity $\vec{U}(t)$ (1.2) is to be replaced by

$$\vec{U}_{magn} = \vec{V} - \vec{v}_c - \delta_{\perp} \vec{v}_{\perp}^0. \quad (2.21)$$

Here $\vec{v}_c \parallel \vec{B}$ is the velocity of the electron Larmor circle center (Fig. 2). This formula takes into account the peculiarity of the motion of the “magnetized” electron,

whose time-averaged displacement across a (ideal homogeneous) magnetic field is equal to zero (formula (2.16)), whereas the motion along the field line is unlimited (until the electron leaves the electron cooling system). Therefore, instead of formula (1.6), we obtain

$$\vec{F}^{magn} = -Q L_{magn} \int_{\vec{v}} \frac{\vec{U}_{magn}}{|\vec{U}_{magn}|^3} \cdot f(\vec{v}) \cdot d^3 \vec{v},$$

$$L_{magn} = \ln \frac{\rho_{magn}}{\rho_{crit}}. \quad (2.22)$$

The impact parameter ρ_{magn} is actually defined in formula for ρ_{max} (1.11) with the velocity U replaced by U_{magn} (2.21), and now we have

$$\rho_{magn} = \min\{R_{shield}, R_{flight}, a_e\}_{U=U_{magn}}, \quad (2.23)$$

$$R_{shield} = \max\{R_D, R_z\}, \quad R_D = \frac{U_{magn}}{\omega_e},$$

$$R_{flight} = U_{magn} \cdot \tau_{flight}.$$

Replacement of ρ_{min} by ρ_{crit} is evident: it is the lower boundary of the magnetized collisions.

In the case of the axially symmetric ($\Delta_x = \Delta_y = \Delta_{\perp}$) flattened Maxwellian distribution (1.15) we can apply the calculation technique used in Section 1, i.e., “Shemyakin’s trick”. Now formulas (1.16)–(1.20) for magnetized collisions can be written in the dimensionless form

$$F_{\perp}^{magn} = \frac{4Q V_{\perp}}{\sqrt{\pi} \Delta_{\perp}^3} L_{magn} Int_{\perp}^{magn},$$

$$F_{\parallel}^{magn} = \frac{4Q V_{\parallel}}{\sqrt{\pi} \Delta_{\perp}^3} L_{magn} Int_{\parallel}^{free}, \quad (2.24)$$

$$Int_{\perp}^{magn} = \int_0^{\chi_{max}} e^{-\psi_{magn}(\chi, x, y)} \cdot \frac{\chi^2 d\chi}{(1+2(\delta_{\perp}\chi)^2)^2 \sqrt{1+2(\delta_0\chi)^2}},$$

$$Int_{\parallel}^{magn} = \int_0^{\chi_{max}} e^{-\psi_{magn}(\chi, x, y)} \frac{\chi^2 d\chi}{(1+2(\delta_0\chi)^2)^{3/2} (1+2(\delta_{\perp}\chi)^2)},$$

$$\psi_{magn}(\chi, x, y) = \chi^2 \cdot \left(\frac{x^2}{1+2(\delta_{\perp}\chi)^2} + \frac{y^2}{1+2(\delta_0\chi)^2} \right), \quad \delta_0 = \frac{\Delta_{\parallel}}{\Delta_{\perp}}.$$

The variables $x = \frac{V_{\perp}}{\Delta_{\perp}}$ and $y = \frac{V_{\parallel}}{\Delta_{\perp}}$ are the transverse and longitudinal ion velocity components normalized to Δ_{\perp} . The parameter δ_{\perp} (2.20) depends on the impact parameter.

For estimates one can use its ρ -averaged value

$$\begin{aligned} \langle \delta_{\perp} \rangle_{\rho} &= \frac{1}{\pi \rho_{\text{magn}}^2} \cdot 2\pi \int_{\rho_{\text{crit}}}^{\rho_{\text{magn}}} \delta_{\perp}(\rho) \cdot \rho \cdot d\rho = \\ &= \frac{2\omega_L \rho_{\text{crit}}^3}{U_{\text{magn}} \rho_{\text{magn}}^2} \int_1^{\zeta_{\text{max}}} \left(\sqrt{1 + \frac{2}{\zeta^3(\zeta^3+4)}} - 1 \right) \zeta \cdot d\zeta, \quad (2.25) \\ \zeta_{\text{max}} &= \frac{\rho_{\text{magn}}}{\rho_{\text{crit}}} \gg 1. \end{aligned}$$

The dimensionless upper limit in the integrals in (2.24) is infinity, i.e., chosen as $\chi_{\text{max}} \gg 1$. In the numerical calculations below we used $\chi_{\text{max}} = 20$.

The numerical examples are given in Sections 3–5. At $\zeta_{\text{max}} \gg 1$ the integral in (2.25) can be approximately calculated as

$$\begin{aligned} \text{Int}_{\rho} &\approx \int_1^{\zeta_{\text{max}}} \frac{d\zeta}{\zeta(\zeta^3+4)} = -\frac{1}{12} \cdot \ln \left(1 + \frac{4}{\zeta^3} \right) \Big|_1^{\zeta_{\text{max}}} = \\ &= \frac{\ln 5}{12} = 0.134 \end{aligned}$$

and

$$\langle \delta_{\perp} \rangle_{\rho} \approx 2 \frac{\omega_L \rho_{\text{crit}}^3}{U_{\text{magn}} \rho_{\text{magn}}^2} \cdot 0.134. \quad (2.26)$$

2.3 Friction force at free collisions in magnetic field

At free electron-ion collisions, i.e. at impact parameters $\rho_{\text{min}} < \rho < \rho_{\text{crit}}$, the cooling friction force is described by formula (1.20) from Section 1 (even in the magnetic field!). Only difference is in the Coulomb logarithm that is now equal to

$$L_{\text{free}} = \ln \frac{\rho_{\text{crit}}}{\rho_{\text{min}}}. \quad (2.27)$$

In the approximation of the flattened Maxwellian velocity distribution of electrons (1.15) we find from (1.20) the “Mathcad’able” formulas for the cooling force

$$\begin{aligned} F_{\perp}^{\text{free}} &= \frac{4Q}{\sqrt{\pi}} \frac{V_{\perp}}{\Delta_{\perp}^3} L_{\text{free}} \text{Int}_{\perp}^{\text{free}}, \\ F_{\parallel}^{\text{free}} &= \frac{4Q}{\sqrt{\pi}} \frac{V_{\parallel}}{\Delta_{\parallel}^3} L_{\text{free}} \text{Int}_{\parallel}^{\text{free}}, \quad (2.28) \\ \text{Int}_{\perp}^{\text{free}} &= \int_0^{\chi_{\text{max}}} e^{-\psi_{\text{free}}(\chi, x, y)} \cdot \frac{\chi^2 d\chi}{(1+2\chi^2)^2 \sqrt{1+2(\delta_0 \cdot \chi)^2}}, \end{aligned}$$

$$\text{Int}_{\parallel}^{\text{free}} = \int_0^{\chi_{\text{max}}} e^{-\psi_{\text{free}}(\chi, x, y)} \cdot \frac{\chi^2}{(1+2(\delta_0 \cdot \chi)^2)^{3/2} (1+2\chi^2)},$$

$$\psi_{\text{free}}(\chi, x, y) = \chi^2 \cdot \left(\frac{x^2}{1+2\chi^2} + \frac{y^2}{1+2(\delta_0 \cdot \chi)^2} \right).$$

All the symbols δ_0 , x , y , χ_{max} are defined in the description of the details of formulas (2.24) and (2.25) above.

One should emphasize that the basis for the application of the results of Section 1 and, particularly, formulas (1.3)–(1.5) to equation (2.9) is that this equation has no terms containing (or connected to) the magnetic field \vec{B} .

3 Zones of the electron cooling regimes and the criterion of magnetization

To illustrate the cooling force analyses described above we present the results of the numerical simulation performed for two sets of electron cooler parameters — nonrelativistic (“NAP-M experiment”) and relativistic (“NICA project”).

Table 1. Parameters of two electron cooling system.

Electron cooler	a) NAP-M experiment [8, 9]	b) NICA project [17]
Ring circumference, m	48.0	503.0
Ratio of the cooling section length to the ring circumference, η	0.02	0.012
Type of particles to be cooled	proton	$^{197}\text{Au}^{79+}$
Electron energy, MeV	0.03	2.5
Electron current, Amp	0.3	1.0
Electron beam radius, cm	0.5	1.0
Electron density in PRF, cm^{-3}	2.3×10^8	1.1×10^7
Electron temperature in PRF, eV, T_{\perp}	0.1	0.2
T_{\parallel}	8.8×10^{-5}	3.2×10^{-5}
Ratio $\Delta_{\parallel}/\Delta_{\perp}$	0.03	0.013
Longitudinal magnetic field, kG	1.0	2.0

Above we formulated the necessary and sufficient conditions of magnetization (2.11)–(2.13). These conditions divide the entire area of the impact parameters in two zones (Fig. 4):

- zone of free collisions, $\rho_{\text{min}} \leq \rho < \rho_{\text{crit}}$,
- zone of magnetized collisions, $\rho_{\text{crit}} \leq \rho \leq \rho_{\text{max}}$.

In Fig. 4–7, 9, and 10 the velocity components are normalized to Δ_{\perp} and are equal to each other: $V_{\parallel} = V_{\perp}$, i.e. $x(V_{\perp}) = y(V_{\parallel})$.

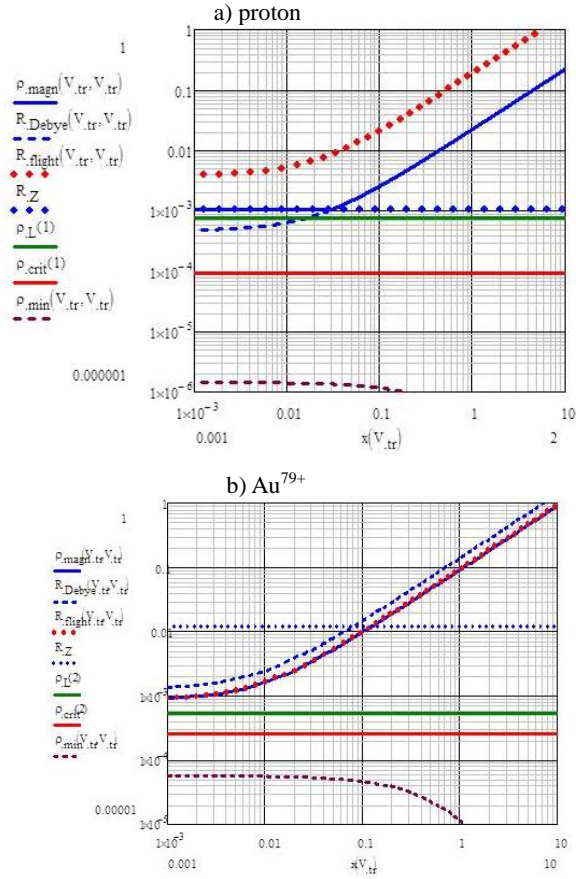


Fig. 4 Dependence of the impact parameters on the ion velocity: ρ_{magn} (blue curve), R_{Debye} (blue dashed curve), R_{flight} (red dotted curve), R_z (blue dotted curve), ρ_L (green curve), ρ_{crit} (red curve), ρ_{min} (dark red dashed line).

Figure 5 demonstrates how the parameter N_ρ (2.18) depends on the impact parameter. In the zone of magnetized collisions (above the red curve in Fig. 5) we find $N_\rho > 1$ in a certain range of the impact parameter ρ for both “NAP-M” and “NICA” parameters. A more complicated case is at free collisions: for “NAP-M” $N_\rho < 1$ below ρ_{crit} , whereas for “NICA” there is area of free collisions with $N_\rho > 1$. However, as we will see below, the contribution of the free collisions to the friction force significantly yields to the contribution of the magnetized collisions at reasonable magnitude of the magnetic field (see criterion (3.2) below).

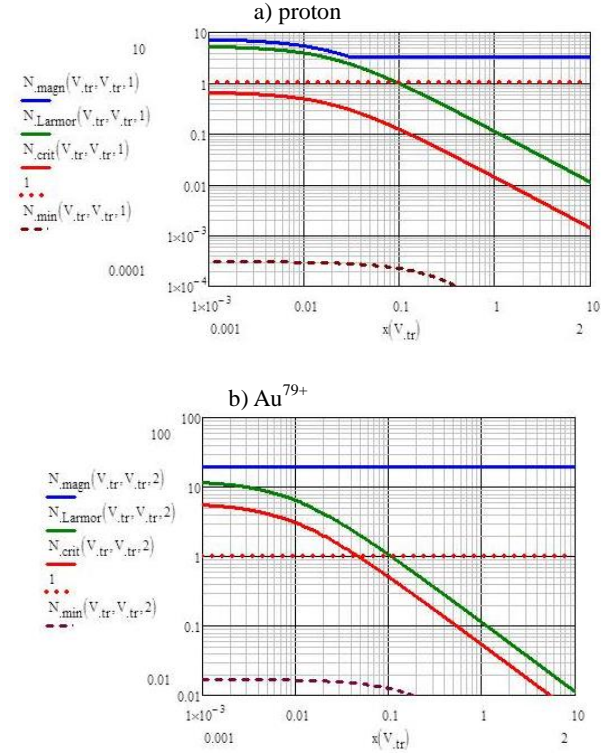


Fig. 5 Dependence of N_ρ on the ion velocity for four critical impact parameters: $N_\rho(\rho_{magn}, x)$ (blue curve), $N_\rho(\rho_{Larmor}, x)$ (green curve), $N_\rho(\rho_{crit}, x)$ (red curve), $N_\rho = 1$ (red dotted curve), and $N_\rho(\rho_{min}, x)$ (dark red dashed curve).

The magnetization efficiency can be characterized by the ratio of the Coulomb logarithms

$$L_{magn}/L_{free} = k > 1. \quad (3.1)$$

Using expressions for L_{magn} (2.21) and L_{free} (2.25), one can “extract” from equality (3.1) the minimal value of the field B necessary for magnetization of the cooling electrons with the efficiency k

$$B_{magn} \approx \frac{ze}{(\rho_{magn} \cdot \rho_{min}^k)^{2/(k+1)}} \cdot \frac{c}{v_\perp}. \quad (3.2)$$

This, rather intricate, expression shows that B_{magn} is determined by ρ_{magn} and ρ_{min} , which in turn depend on the ion velocity (Fig. 6).

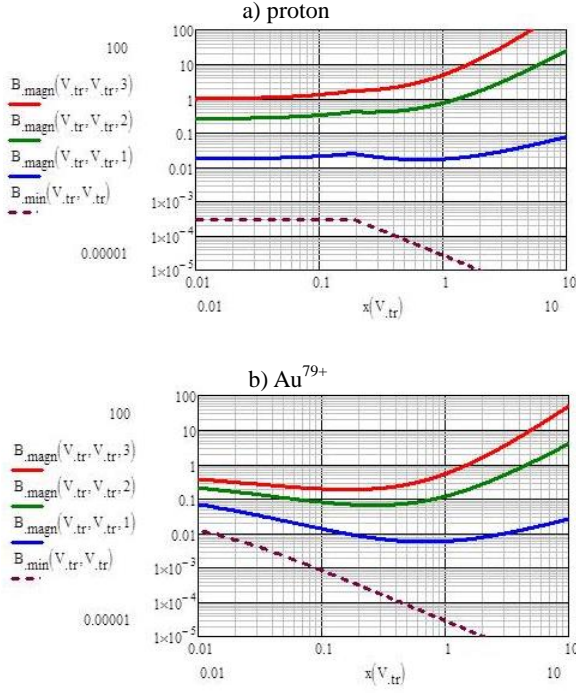


Fig. 6 Dependence of B_{magn} (3.2) on the normalized ion velocity $x = y$ at $k = 1$ (blue curve), 2 (green curve), 3 (red curve); the same dependence for B_{min} (2.13) (dark red dashed curve).

4 New formulas for friction force

The analysis carried out above shows that the friction force of the electron cooling can be described by a formula consisting of two parts

$$\vec{F}_{cool} = \vec{F}_{free} + \vec{F}_{magn}. \quad (4.1)$$

In the case of the flattened Maxwellian velocity distribution of electrons (1.15) the components of \vec{F}_{magn} are described by (2.24) and those of \vec{F}_{free} by (2.28). These formulas are used for numerical simulation here and in the next section. We calculate the friction force at different values of the parameters, but at a certain restriction, namely, the equality of the ion velocity components $V_{\parallel} = V_{\perp} \equiv V$ (Fig. 7). This restriction results from the limited computational capability of the Mathcad code used by the author. Nevertheless, it does not prevent us from analyzing the main features of the cooling friction force. Particularly, one should underline the character of the friction force—strong dependence of the force $F_{cool}(\vec{V})$ function on the ratio of V_{\parallel}/V_{\perp} (Fig. 8).

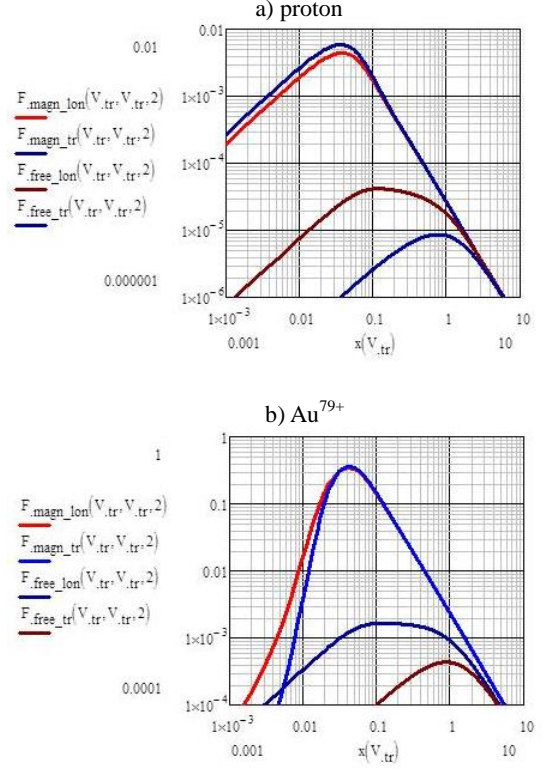


Fig. 7 Dependence of the longitudinal and transverse components of the friction force on the ion velocity for magnetized and free collisions: $F_{\parallel}^{magn}(x)$ (red curve), $F_{\perp}^{magn}(x)$ (blue curve), $F_{\parallel}^{free}(x)$ (dark red curve), $F_{\perp}^{free}(x)$ (dark blue curve).

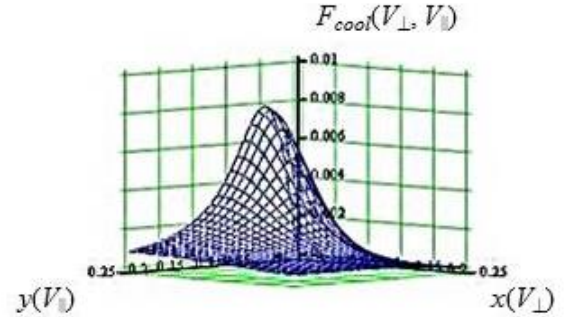


Fig. 8 Dependence of the transverse component of the friction force (4.1) on the normalized ion velocity components x and y (arbitrary units) (NAP-M experiment).

It is also worth noting that here and below, for the sake of convenience, in the figures show the modulus of $F_{cool}(\vec{V})$, although actually $\vec{F}_{cool}(\vec{V}) < 0$ at $\vec{V} > 0$ and vice versa.

Figure 7 shows the difference of the features of the friction force at magnetized and free collisions. Both are calculated for the flattened electron velocity distribution

(1.15) at the ratio $\Delta_{\parallel}/\Delta_{\perp} = 0.03$ (NAP-M) and 0.013 (NICA). Due to this “flatness” of $f(\vec{v})$, the friction force components for the magnetized collisions have the maxima at

$$(V_{\perp}^{magn})_{max} \approx (V_{\parallel}^{magn})_{max} \sim \Delta_{\parallel}, \quad (4.2)$$

whereas for free collisions both maxima of the friction force components are significantly shifted to the larger values of the ion velocity components

$$\Delta_{\perp} > (V_{\perp}^{free})_{max} > (V_{\parallel}^{free})_{max} \gg \Delta_{\parallel}. \quad (4.3)$$

This is the peculiarity of the magnetized friction force.

5 VVP formula and comparison with the new formulas

The formula for the friction force was derived by Vasily V. Parkhomchuk in 1978 [6] and became known as the Parkhomchuk formula (“VVP formula” below). It has the following form:

$$\begin{aligned} \vec{F}_{VVP} &= -\frac{Q}{\pi} \cdot \frac{\vec{V}}{[V_{\perp}^2 + V_{\parallel}^2 + V_{eff}^2]^{\frac{3}{2}}} \cdot L_{VVP}, \\ L_{VVP} &= \ln \left[1 + \frac{(\rho_{max})_{VVP}}{\rho_L + (\rho_{min})_{VVP}} \right], \\ V_{eff} &= \sqrt{\Delta_{\parallel}^2 + (\gamma\beta c\theta_B)^2}, \\ (\rho_{max})_{VVP} &= \frac{\sqrt{V_{\perp}^2 + V_{\parallel}^2} \tau_{flight}}{1 + \omega_e \tau_{flight}}, \\ (\rho_{min})_{VVP} &= \frac{Ze^2}{m(V_{\perp}^2 + \Delta_{\parallel}^2)}. \end{aligned} \quad (5.1)$$

$$(5.2)$$

$\theta_B = \delta B/B$ is the amplitude of the magnetic field ripples in the cooling section.

The new and the VVP formula substantially differ in several properties and parameters. The VVP formula has no difference between the transverse and longitudinal components of \vec{F}_{VVP} in the PRF. It has the coefficient π in the denominator and a different definition of the Coulomb logarithm L_{VVP} . Both differences lead to a decrease in F_{VVP} compared with F_{cool} , which is the most important distinction of the formulas.

The new formulas show a much stronger increase in the friction force than the VVP formula as the parameters change from the NAP-M experiment to the NICA project (compare Fig. 9a and Fig. 9b).

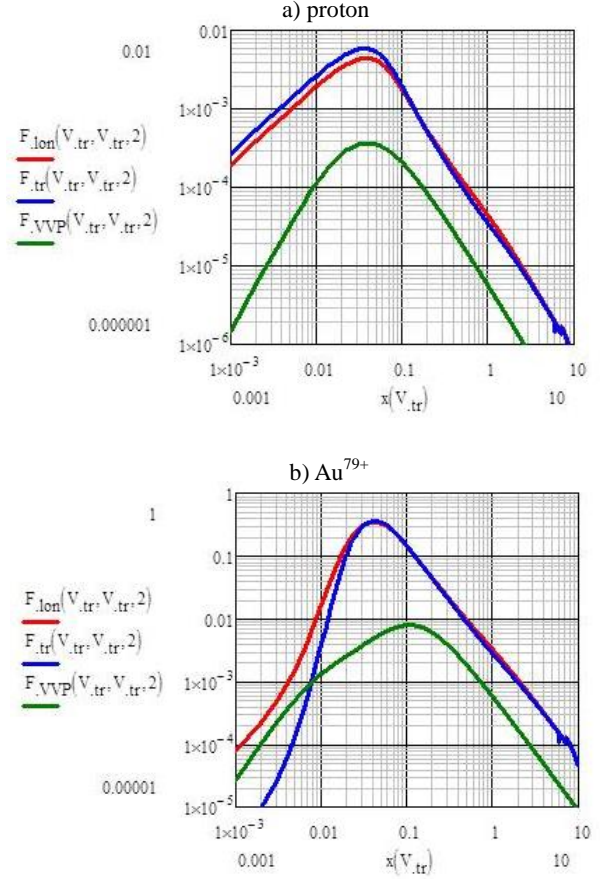


Fig. 9 Comparison of $(F_{cool}(x))_{\parallel}$ (red curve) and $(F_{cool}(x))_{\perp}$ (blue dashed curve) with $F_{VVP}(x)$ (green curve).

The difference of F_{cool} and F_{VVP} vanishes if we replace L_{magn} in (2.24) by L_{VVP} (Fig. 10). Comparing the Coulomb logarithms of new formulas (both $L_{magn}(x)$ (2.22) and $L_{free}(x)$ (2.27)) with one of the VVP formula ($L_{VVP}(x)$ (5.1)), we see (Fig. 11) that the latter is significantly smaller than the former ones and converges to zero in the velocity range $x < 0.1$, i.e., near the maximum of the friction force. That casts a doubt on the correctness of the application of the VVP formula in this velocity range.

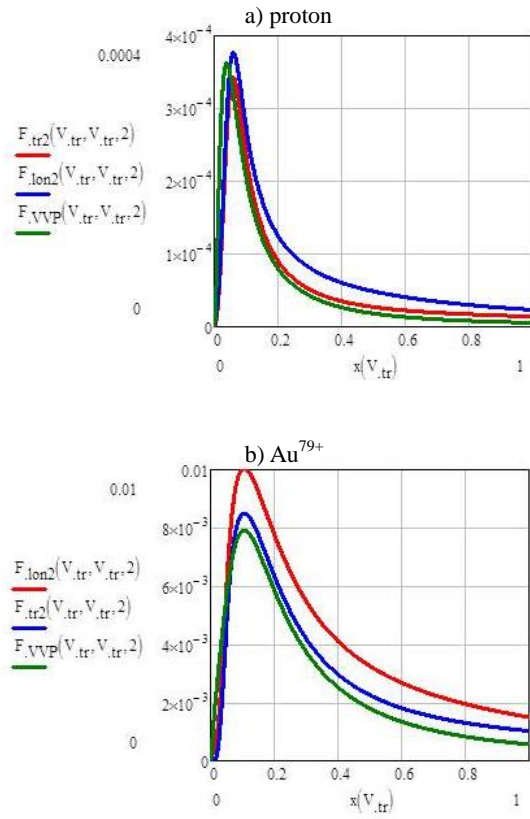


Fig. 10 Comparison of the friction force for the VVP formula $F_{VVP}(x)$ (green curve) with the modified new formulas $F_{\parallel}(x)$ (red curve), $F_{\perp}(x)$ (blue curve) on the linear scale.

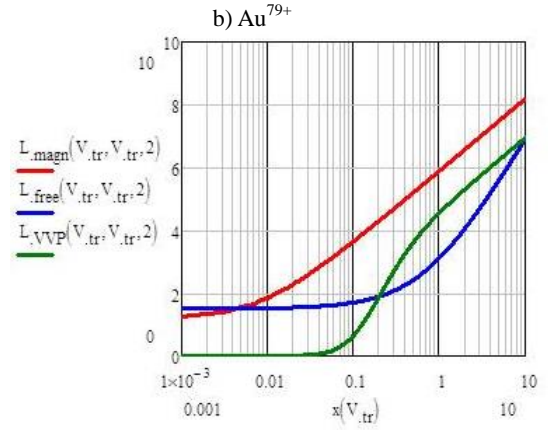
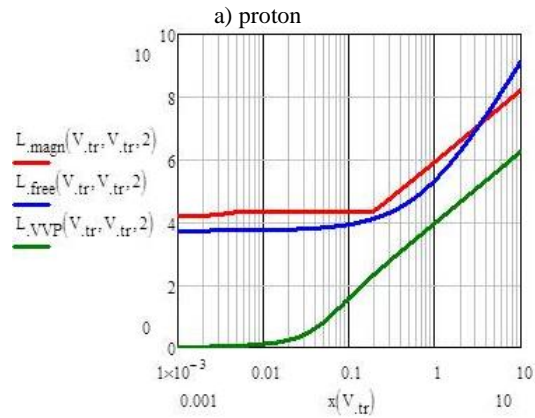
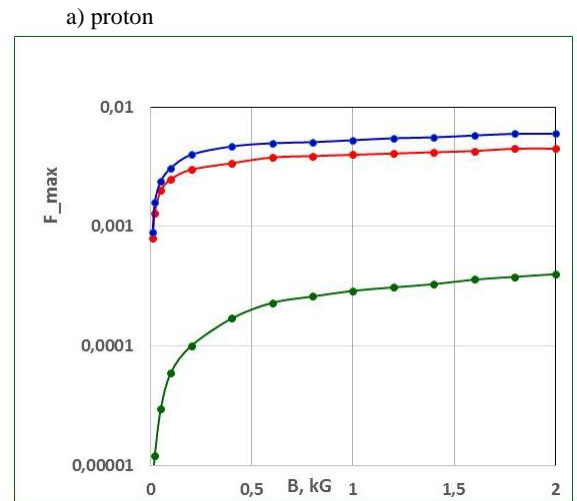


Fig. 11 Dependence of the Coulomb logarithms on the ion velocity $x(V)$ for the new formulas (magnetized (red) and free (blue) collisions) and for the VVP formula.

Dependence of $(F_{cool})_{max}$ on the magnetic field B is substantially different for the new formulas and for the VVP formula (Fig. 12). In the latter F_{max} approaches zero as $B \rightarrow 0$, which contradicts the experimental results. The new formulas are devoid of such weakness. The abrupt falldown could be caused by the absence of free collisions in the VVP formula and a large increase in the Larmor radius (in the denominator of L_{VVP}).



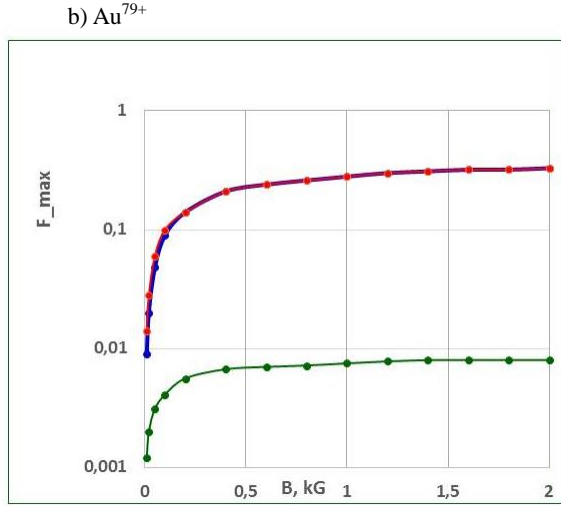


Fig. 12 Dependence of the maxima of the friction force components on the magnetic field B : $(F_{\parallel}(x, B))_{\max}$ (red curve), $(F_{\perp}(x, B))_{\max}$ (blue dashed curve), and $(F_{VVP}(x, B))_{\max}$ (green curve).

Summary and conclusions

1. The presented approach to the analyses and description of the electron cooling friction force allows one to construct a scheme of the force formation based on the solution of the rigorous equations of particle motion in the magnetic field of an electron cooler and the common electron-ion Coulomb field of the interacting particles.
2. The main results of the presented analyses are the following:
 - 2.1. The rigorous equations of particle motion in binary collisions are derived, and it is shown that at certain conditions the equations can be reduced to the two-body problem and the Larmor rotation of the electron violated by the Coulomb field of the ion;
 - 2.3. The zones of impact parameters in magnetized and free collisions are defined;
 - 2.4. An analytic solution applicable to the simplified numerical simulation of the electron cooling process is found;
 - 2.5. The components of the derived formulas depend on both the transverse and the longitudinal component of the ion velocity. Such “coupling” of V_{\perp} and V_{\parallel} requires simultaneous simulation of the cooling process by all three degrees of freedom.

3. The present description of the cooling force is based on analyses of binary collisions of electrons and ions. The electron plasma influence is taken into account as only effect — Debye screening that limits the value of maximal impact parameter. The attempts to find a solution on the basis of the electron plasma approach have not brought any concrete results so far, and the research in this direction needs to be continued.

4. The weak point is certainly the “separation” of the electron velocity distribution and the values of the impact parameters, i.e., the “logarithmic description”. The search for the “nonlogarithmic” solution is an urgent task for the future development of the electron cooling theory.

Acknowledgments

The author is sincerely grateful to Prof. Takeshi Katayma, who initiated this work, to Prof. Marat Eseev for the help in numerical simulations, and to Mrs. Tatyana Stepanova for the preparation of this paper for publication.

Annex I. Elastic collisions in two-body problem

The following equations are written on the basis of the momentum and energy conservation laws for two particles in elastic collisions

$$\vec{p}_1 + \vec{p}_2 = \vec{p}_1^0 + \vec{p}_2^0, \quad (\text{I.1})$$

$$\varepsilon_1 + \varepsilon_2 = \varepsilon_1^0 + \varepsilon_2^0. \quad (\text{I.2})$$

Here zero superscripts indicate the initial (before collision) values of the parameters of two colliding particles. From these equations there obviously follow equalities of momentum and energy changes in the collision

$$\Delta p = \vec{p}_1 + \vec{p}_1^0 = -(\vec{p}_2 - \vec{p}_2^0), \quad (\text{I.3})$$

$$\Delta \varepsilon = \varepsilon_1 - \varepsilon_1^0 = -(\varepsilon_2 - \varepsilon_2^0). \quad (\text{I.4})$$

Now we can consider an elastic collision of two particles interacting via a central force $\vec{F}(\vec{r})$ — the well-known two-body problem (Fig. I.1).

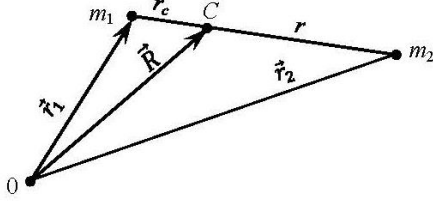


Fig. I.1 Scheme of interaction of two point-like particles m_1 and m_2 ; \vec{r}_1 , \vec{r}_2 are the radius-vectors of the particles, C is the center of mass of two particles, \vec{R} is its radius-vector, and 0 is the reference point.

$$\vec{r}_c = \frac{m_2}{m_1 + m_2} \cdot \ll r \text{ at } m_2 \ll m_1.$$

The equations of motion of two nonrelativistic particles have the form

$$\begin{aligned} m_1 \ddot{\vec{r}}_1 &= \vec{F}(\vec{r}), \\ m_2 \ddot{\vec{r}}_2 &= -\vec{F}(\vec{r}), \\ \vec{r} &= \vec{r}_1 - \vec{r}_2. \end{aligned} \quad (\text{I.5})$$

Here $m_{1,2}$ and $\vec{r}_{1,2}$ are the masses and the radius-vectors of the particles.

The first two equations in (I.5) give us

$$\ddot{\vec{r}}_1 - \ddot{\vec{r}}_2 = \left(\frac{1}{m_1} + \frac{1}{m_2} \right) \cdot \vec{F}(\vec{r}),$$

or

$$\mu \ddot{\vec{r}} = \vec{F}(\vec{r}), \quad \mu = \left(\frac{1}{m_1} + \frac{1}{m_2} \right)^{-1}. \quad (\text{I.6})$$

The parameter μ is the so-called reduced mass. Thus, the relative motion of two particles is described by the equation of motion of the particle with mass μ under the action of the force $\vec{F}(\vec{r})$. It is worth mentioning that the sum of the first two equations in (I.5) gives us the momentum conservation law

$$m_1 \ddot{\vec{r}}_1 + m_2 \ddot{\vec{r}}_2 = 0.$$

Integrating this equality, we arrive at equation (I.1).

As a result of the collision with duration τ , the momentum of the μ -particle changes by the value

$$\Delta \vec{p}_\mu = \int_0^\tau \vec{F}(\vec{r}(t)) \cdot dt. \quad (\text{I.7})$$

The quantity $\Delta \vec{p}_\mu$ is connected with the parameter Δp by the following “chain” of the evident equalities:

$$\Delta \vec{p}_\mu \equiv \mu(\dot{\vec{r}} - \dot{\vec{r}}_0) = \mu[\vec{V}_1 - \vec{V}_2 - (\vec{V}_1^0 - \vec{V}_2^0)] =$$

$$= \mu \left(\frac{\Delta \vec{p}_1}{m_1} - \frac{\Delta \vec{p}_2}{m_2} \right) = \Delta \vec{p}.$$

Thus, in the collision either of the two colliding particles suffers the momentum change

$$\Delta \vec{p} = \Delta \vec{p}_1 = -\Delta \vec{p}_2 = \Delta \vec{p}_\mu. \quad (\text{I.8})$$

Annex II. Charged particle in the crossed homogeneous magnetic and central Coulomb fields

We consider motion of a charged particle (e, m) in cross fields — homogeneous magnetic \vec{B} and central Coulomb $\vec{E}(\vec{r})$ ones. The latter is chosen in the approximate form

$$\vec{E}(\vec{r}) = \frac{Ze^2}{mp^3} \cdot \vec{r}_\perp, \quad \vec{r}_\perp = \{x, y\}. \quad (\text{II.1})$$

This approximation is valid in the case of magnetized collisions when condition (2.12) is met. Then we will analyze the particle trajectory in the plane transverse to the magnetic field line using a specific choice of the coordinate corresponding to Fig. 2. It means that we have to find a solution of equation (2.10). In the PRF coordinates (x, y) this equation gives the system of two linear differential equations

$$\ddot{x} + \omega_L \dot{y} + \omega_z^2 \cdot x = 0,$$

$$\ddot{y} - \omega_L \dot{x} + \omega_z^2 \cdot y = 0, \quad \omega_L = \frac{eB}{mc}, \quad \omega_z^2 = \frac{Ze^2}{mp^3}. \quad (\text{II.2})$$

The origin of x, y coordinates lies on the field B line that coincides with the axis of the unperturbed (before collisions) Larmor rotation of the particle (Fig. II.1).

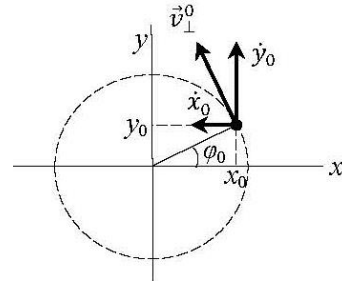


Fig. II.1 Initial position of the particle Larmor rotation trajectory.

Multiplying the second equation by the imaginary unit and adding both equations, we arrive at the equation

$$\ddot{\xi} - i\omega_L \dot{\xi} + \omega_z^2 \cdot \xi = 0, \quad \xi = x + iy. \quad (\text{II.3})$$

The solution of this equation is

$$\xi(t) = A_1 e^{i\omega_+ t} + A_2 e^{i\omega_- t}, \quad (\text{II.4})$$

$$\omega_{\pm} = \frac{\omega_L \pm \Omega}{2}, \quad \Omega \equiv \sqrt{\omega_L^2 + 4\omega_z^2}, \quad (\text{II.5})$$

$$A_1 = -\frac{\omega_- \xi_0 + i\dot{\xi}_0}{\sqrt{\omega_L^2 + 4\omega_z^2}}, \quad A_2 = \frac{\omega_+ \xi_0 + i\dot{\xi}_0}{\sqrt{\omega_L^2 + 4\omega_z^2}}. \quad (\text{II.6})$$

Here $\xi_0 = \xi(0)$ and $\dot{\xi}_0 = \dot{\xi}(0)$. Substituting amplitudes (II.5) in solution (II.3) and separating the real and imaginary parts of $\xi(t)$, we find

$$\begin{aligned} x(t) = & \frac{1}{\Omega} \cdot \{x_0(\omega_+ \cos \omega_- t - \omega_- \cos \omega_+ t) + \\ & + \dot{x}_0(\sin \omega_+ t - \sin \omega_- t) - y_0(\omega_+ \sin \omega_- t - \omega_- \sin \omega_+ t) + \\ & + \dot{y}_0(\cos \omega_+ t - \cos \omega_- t)\}, \quad (\text{II.7}) \\ y(t) = & \frac{1}{\Omega} \cdot \{x_0(\omega_+ \sin \omega_- t - \omega_- \sin \omega_+ t) - \\ & - \dot{x}_0(\cos \omega_+ t - \cos \omega_- t) + y_0(\omega_+ \cos \omega_- t - \omega_- \cos \omega_+ t) + \\ & + \dot{y}_0(\sin \omega_+ t - \sin \omega_- t)\}. \end{aligned}$$

The particle trajectory in the (x, y) plane can be calculated with these formulas at the given frequencies ω_{\pm} (II.5) and initial conditions (Fig. 3). The radial size of the trajectory oscillates in time, as follows from (II.7):

$$r(t) = \sqrt{x^2(t) + y^2(t)} = r_0 \sqrt{1 + \frac{4\omega_z^2}{\Omega^2} \cdot \sin^2 \frac{\Omega t}{2}}. \quad (\text{II.8})$$

Thus, the radial displacement of the particle in the collision is limited

$$r_0 \leq r(t) \leq r_0 \sqrt{1 + \frac{4\omega_z^2}{\Omega^2}}. \quad (\text{II.9})$$

For the description of the electron-ion collision (Section 2) we need to know time dependence of the transverse

electron velocity. It can be found from equations (II.7) by the following obvious procedure:

$$\begin{aligned} (v_{\perp}(t))^2 = & (\dot{x}(t))^2 + (\dot{y}(t))^2 = 2\omega_z^4(x_0^2 + y_0^2) \times \\ & \times (1 - \cos \Omega t) + (\dot{x}_0^2 + \dot{y}_0^2)[\omega_L^2 + 2\omega_z^2(1 + \cos \Omega t)] - \\ & - 2\omega_z^2[(x_0 \dot{x}_0 + y_0 \dot{y}_0)\Omega \cdot \sin \Omega t - (x_0 \dot{y}_0 - y_0 \dot{x}_0) \times \\ & \times \omega_L(1 - \cos \Omega t)]. \quad (\text{II.10}) \end{aligned}$$

This intricate equation can be appreciably simplified by assuming that the initial coordinates and the velocity of the particle correspond to its unperturbed Larmor rotation. Then (Fig. II.1) we have the following relations between the initial coordinates and the velocity of the particle:

$$v_{\perp}^0 = \omega_L r_0 = \omega_L \sqrt{x_0^2 + y_0^2}, \quad (\text{II.11})$$

$$\dot{x}_0 = -\omega_L y_0, \quad \dot{y}_0 = \omega_L x_0.$$

These conditions give us the following equalities:

$$x_0 \dot{x}_0 + y_0 \dot{y}_0 = 0, \quad x_0 \dot{y}_0 - y_0 \dot{x}_0 = v_{\perp}^0 r_0^0,$$

and we finally come to the particle velocity in the presence of the central electric field (II.1)

$$v_{\perp}(t) = v_{\perp}^0 \sqrt{1 + 4 \frac{\omega_z^4}{\omega_L^2 \Omega^2} \cdot \sin^2 \frac{\Omega t}{2}}. \quad (\text{II.12})$$

Calculating the time-averaged square of the velocity $v_{\perp}(t)$, we obtain

$$\sqrt{\overline{v_{\perp}^2}} = v_{\perp}^0 \sqrt{1 + \alpha}, \quad \alpha \equiv \frac{2\omega_z^4}{\omega_L^2(\omega_L^2 + 4\omega_z^2)}. \quad (\text{II.13})$$

References

- 1 Budker G. I. Proc. Intern. Symp. Electron and Positron Storage Rings, Sacley, 1966; Atomic Energy, 1967, **22**: 346.
- 2 Arenshtam A. I., Meshkov I. N., Salimov R. A. and Skriskiy A. N., Journ. of Tech. Physics (Russ.), 1971, **41**: 336.
- 3 Kudelainen V. I., Meshkov I. N. and Salimov R. A. preprint BINP 70-72, 1970; preprint CERN 77-08, part B, CERN, 1977.
- 4 Budker G. I., Dikansky N. S., Kudelainen V. I. et al. Proc. IV Soviet Part. Accel. Conf., Moscow "Nauka", 1975, **2**: 309 (in Russian); Part.

- Accelerators, 1976, **7**: 197; Atomic Energy, 1976, **40**: 49.
- 5 Budker G. I., Bulychev A. F., Dikansky N. S. et al. Proc. V Soviet Part. Accel. Conf., Moscow “Nauka”, 1977, **1**: 236; preprint BINP76-92, 1976; Transl. CERN PS/DL/Note 76-25, 1976.
 - 6 Parkhomchuk V. V. and Skrinsky A. N., PEPAN, 1981, **12**: 557.
 - 7 Derbenev Ya. S. and Skrinsky A. N. Plasma Physics, 1978, **4**: 492.
 - 8 Meshkov I. PEPAN, 1994, **25**: 631.
 - 9 Parkhomchuk V. V. and Skrinsky A. N., Physics-Uspekhi, 2000, **170**: 473.
 - 10 Fedotov A. V. Gällander B., Litvinenko V. N. et al., PhysRev **E**, 2006, **73**: 066503.
 - 11 Fedotov A. V. Bruhwiler D. L. and Sidorin A. O., Proc. of HB2006, Tsukuba, Japan, WEAY04, p.210.
 - 12 Meshkov I. N. The letter to Ya. S. Derbenev, 19.05.2016.
 - 13 Landau L. D. and Lifshitz E. M. Mechanics, Pergamon Press, 1969, § 19, Formula (19.1).
 - 14 Landau L. D. and Lifshitz E. M. Statistical Physics, 3 ed., Pergamon, 1980.
 - 15 Shemyakin A. Fermilab preprint TM-2374-AD, 2007.
 - 16 Bjorken J. B. and Mtingwa S. K., Part. Accelerators, 1983, **13**: 115.
 - 17 Kekelidze V. D., Lednicky R., Matveev V. A., Meshkov I. N., Sorin A. S. and Trubnikov G. V. Eur. Phys. J. **A**, 2016, **52**: 211.